

Propagation of Sound Interacting with the Ocean Floor

Herbert Überall, Juan I. Arvelo and Jianren Yuan

Department of Physics, Catholic University of America
Washington, DC 20064, USA

e-mail: HERSHEY@CUA.EDU

Observed cases of residual intensities between convergence zones of propagating underwater sound, in the absence of a bottom slope must be explained, and are illustrated here, by the effects of sound penetrating into the ocean floor and returned back into the water column by the presence of an upward-refracting bottom sound speed gradient. It is shown that depending on the geometry and the bottom properties, this mechanism can lead to quite dramatic examples of inter-convergence zone residuals, providing an interpretation of observed effects of this kind.

1. Introduction

In the deep ocean, sound from an underwater source is channeled in the SOFAR channel to form a long series of convergence zones. These may appear in close pairs, due to surface reflections, and they may also be influenced by bottom reflections when the propagation occurs down a sloping ocean floor [Carey (1986)]. This latter phenomenon may lead to "downslope conversion" of the channeled field, causing residual intensities (of the order of 10dB excess) between convergence zones, as shown in the experiments of Carey. However, when analyzed by a parabolic-equation (PE) model which did not adequately treat the bottom interaction of sound, not all the data could be explained by this mechanism.

Bottom interaction and bottom penetration effects may, however, be invoked for an explanation of residual intensities between convergence zones. The presence of bottom penetration effects from a flat, deep (4000m) ocean floor, has been conclusively established in pulse-

return experiments [Christensen et al. (1975)], especially at lower frequencies (20-200 Hz) where the bottom loss is smallest. These returns, present for flat or sloping ocean floors, are possible if an upward-refracting sound speed gradient prevails in the deep ocean sediments; the presence of such is a well-established fact [Officer (1955)]. Figure 1 demonstrates the presence of bottom refracted rays in the water column, based on the sound velocity profile shown at the left (the sound velocity gradient in the sediment varying from 1536m/s to 1642 m/s). Deeply penetrating rays (to the left of the arrow) are lost by bottom absorption, but shallower rays re-emerge and cause residual intensities between convergence zones. The figure does not show rays that do not reach the bottom, or that merely get reflected by it.

2. Bottom Refraction Effects in Deep Ocean of Constant Depth

A CONGRATS ray tracing program used by us for the non-penetrating rays from a 250-m deep source indicates the presence of a convergence zone at 70-km range,

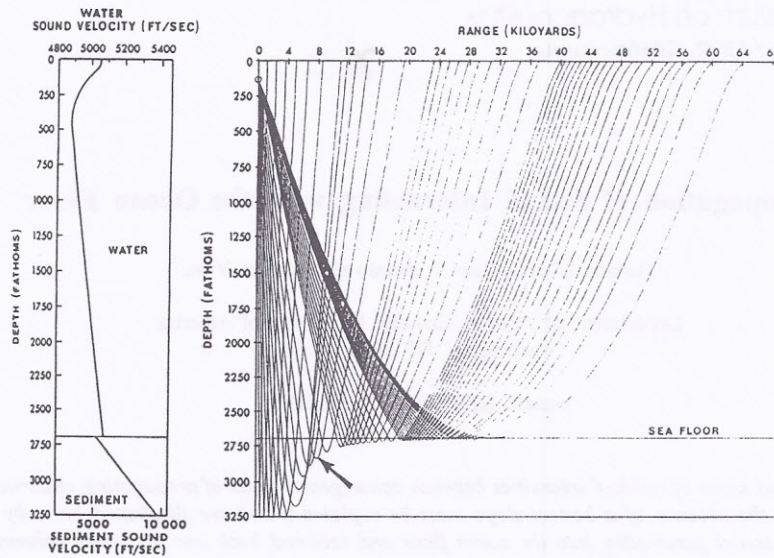


Fig. 1. Deep-ocean water and bottom sound speed profiles, and ray diagram for bottom penetrating rays. From Christensen et al (1975).

based on the sound speed profiles of Fig. 1. A calculation of transmission loss was done by us using the KRAKEN normal-mode model [Porter (1990)]. The results, shown in Fig. 2 (heavy curve) actually indicate the presence of three convergence peaks, at 40, 65 and 85 km range, of which those at 40 and 85 km should be attributable to bottom refracted sound energy.

To verify this interpretation, we repeated the calculation but this time keeping the sediment sound speed constant (equal to the sound speed at the water-bottom interface) in order to eliminate any refracted sound fields. The corresponding light curve in Fig. 2 indeed now only shows the 65-km convergence zone, proving that the peaks at 40 and 85 km are due to bottom refraction. For longer ranges, corresponding results are shown in Fig. 3, indicating a filling-in of inter-convergence zone fields by bottom refraction.

3. Bottom Refraction Effects in an Ocean of Intermediate Depth

We now look for corresponding bottom penetration effects in a lees deep (1650m)

ocean with bottom-limited sound propagation. It was found that here, bottom reflection effects already cause substantial filling-in of convergence zones, but that this filling-in is augmented by bottom refraction. The profile we assume is the same as that of Fig. 1 up to the new depth, and we shall show here results for an upward-refracting bottom gradient simulated by four constant-speed layers up to 1750m depth (Fig. 4). The transmission loss calculation was carried out using the CENTRO/ANTS code developed at Catholic University [Arvelo (1989)]. This code allows for both compressional and shear waves in the sediment, and we assume a sound speed increasing from 1780m/s to 2000m/s in the layers down to the substrate, and a shear speed from 800m/s to 1000m/s.

Figure 5 shows a ray diagram for the water-borne (surface-and bottom-reflected) rays which leads to a convergence zone at 18 km in this case. The layered bottom structure allows only the bottom-penetrating rays to return which left the 250m deep source at angles between -30° and -40° , lying in a shaded band in Fig. 5. The

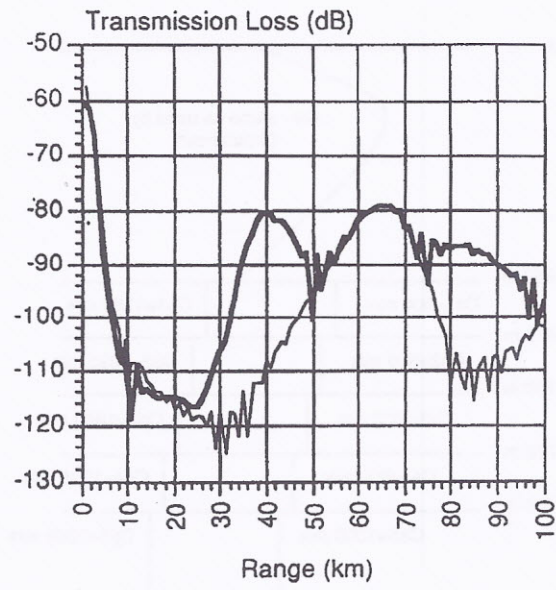


Fig. 2. Transmission loss calculation at 20Hz for source and observer at 250 m depth, based on deep-ocean profiles of Fig. 1 (heavy curve), and on a constant sediment sound speed (light curve).

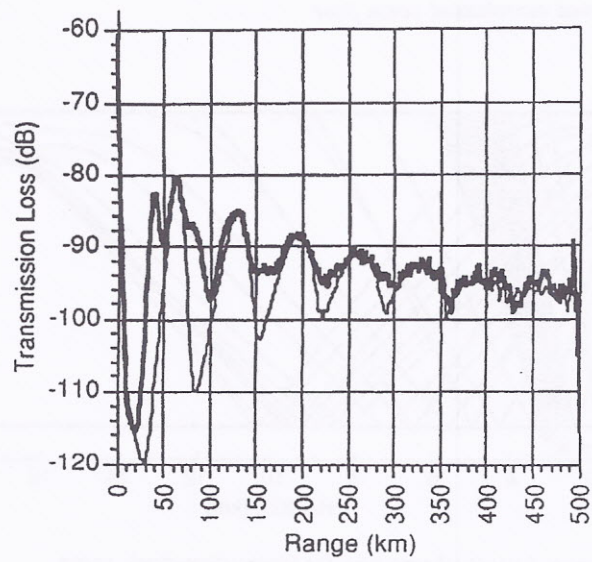


Fig. 3. As in Fig. 2, for ranges out to 500 km.

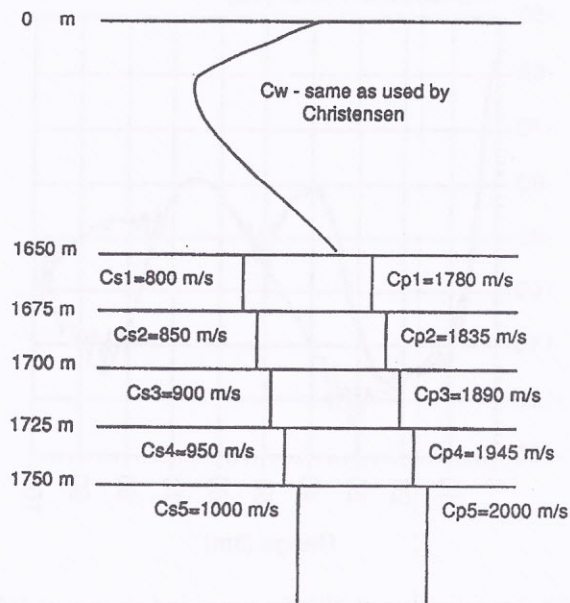


Fig. 4. Multi-layered consolidated ocean floor.

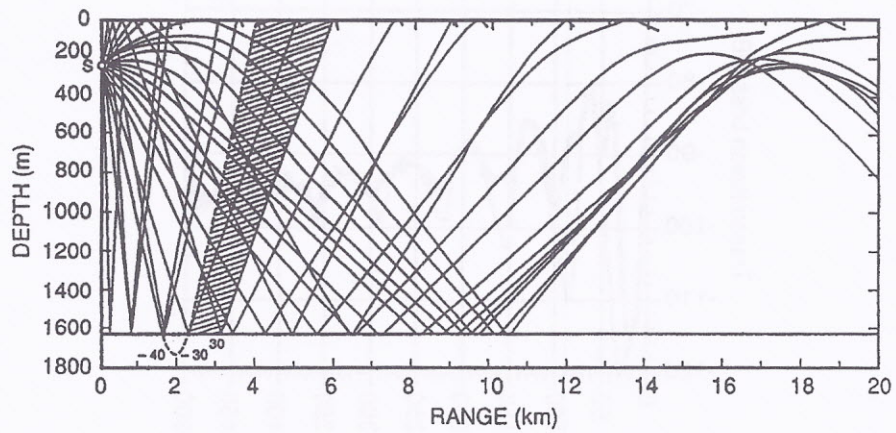


Fig. 5. Ray diagram for water-borne rays for intermediate-depth ocean.

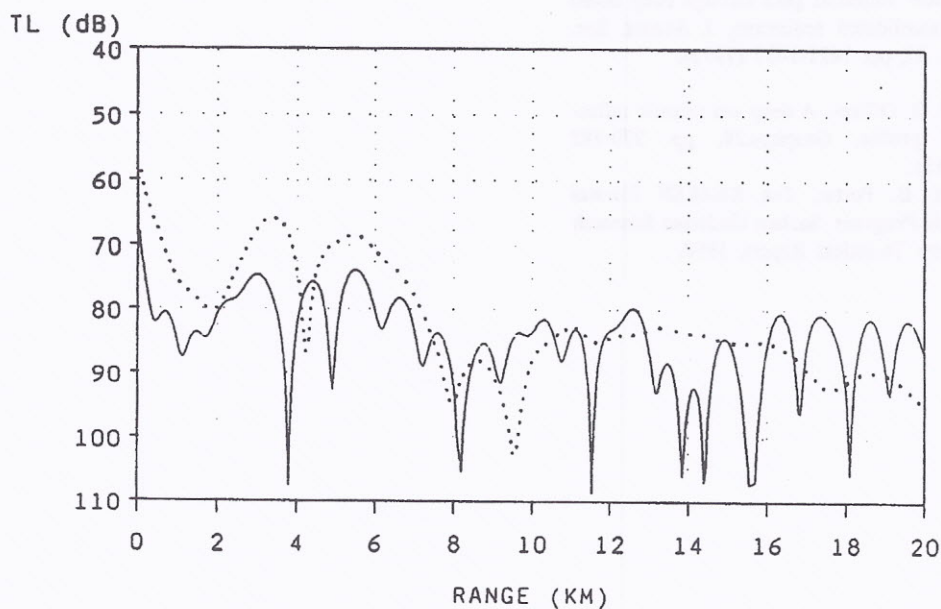


Fig. 6. As in Fig. 2, for an ocean of intermediate depth (solid curve: upward-refracting bottom; dotted curve: constant bottom sound speed).

transmission-loss calculation is shown in Fig. 6 where the dotted curve corresponds to a liquid bottom with constant sound speed 1500.8m/s as the bottom value of the profile (no refracted returns), and the solid curve to the mentioned layered upward-refracting bottom of Fig. 4. It is seen that in this case, bottom refraction generates copious interference effects of the bottom-returned rays with the water-borne rays of Fig. 5.

4. Conclusions

Our normal-mode calculations have demonstrated that interactions of ocean-propagating sound with the ocean floor not only takes place in the form of reflections from the interface, but to a large measure in bottom penetration of the sound, and especially its return into the water column in the presence of an upward-refracting bottom sound velocity gradient as it is often present in the ocean floor sediment layers.

5. Acknowledgements

This research was sponsored by the Office of Naval Technology, United States Navy, for which our profound gratitude is expressed to Dr. R. D. Doolittle.

Reference

- J. I. Arvelo, *Adiabatic Normal-Mode Theory of Low-Frequency Sound Transmission in a Shallow Range-Dependent Ocean with Seismo-Acoustic Effects from the Elastic Bottom Sediments*, Ph.D Dissertation, Catholic University of America (1989).
- W. M. Carey, Measurement of down-slope propagation from a shallow source to a deep ocean receiver, *J. Acoust. Soc. Am.* 79, pp. 49-59 (1986).
- R. E. Christensen, J. A. Frank and W. H. Geddes, Low-Frequency propagation via

shallow refracted path through deep ocean unconsolidated sediments, *J. Acoust. Soc. Am.* 57, pp. 1421-1427 (1975).

C. B. Officer, A deep sea seismic reflection profile, *Geophys.* 20, pp. 270-282 (1955).

M. B. Porter, *The KRAKEN Normal Mode Program*, Saclant Undersea Research Centre Technical Report, 1990.

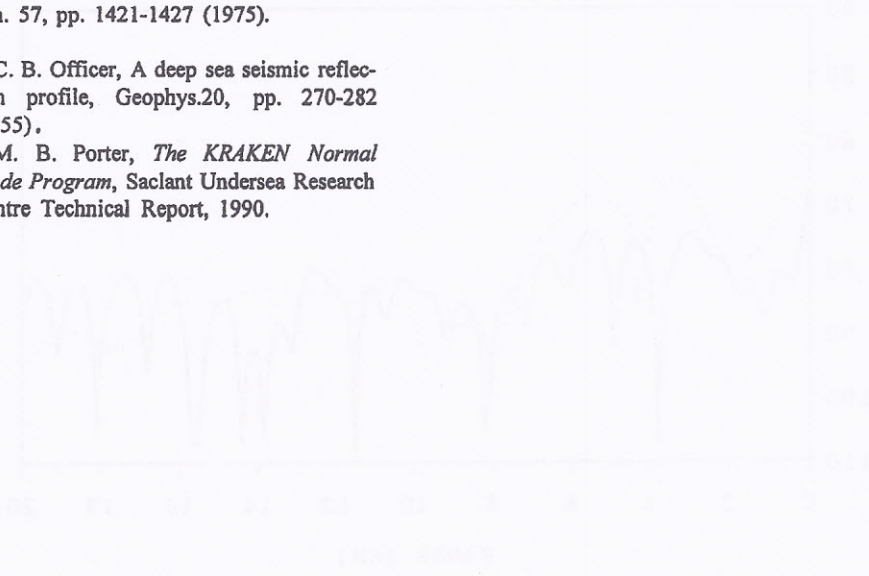


FIG. 1. A typical seismic reflection profile showing multiple reflections from the ocean floor and subsurface layers.

The seismic reflection profile shown in Figure 1 is a typical example of a deep sea seismic reflection profile. It shows multiple reflections from the ocean floor and subsurface layers. The profile is characterized by a series of peaks and troughs, with the highest peak occurring around 35 minutes. The reflections are caused by the interaction of seismic waves with the ocean floor and subsurface layers, which have different acoustic properties. The profile is used to study the structure of the ocean floor and subsurface layers, and to estimate the depth of the ocean floor and the thickness of the subsurface layers.

The seismic reflection profile shown in Figure 1 is a typical example of a deep sea seismic reflection profile. It shows multiple reflections from the ocean floor and subsurface layers. The profile is characterized by a series of peaks and troughs, with the highest peak occurring around 35 minutes. The reflections are caused by the interaction of seismic waves with the ocean floor and subsurface layers, which have different acoustic properties. The profile is used to study the structure of the ocean floor and subsurface layers, and to estimate the depth of the ocean floor and the thickness of the subsurface layers.

The seismic reflection profile shown in Figure 1 is a typical example of a deep sea seismic reflection profile. It shows multiple reflections from the ocean floor and subsurface layers. The profile is characterized by a series of peaks and troughs, with the highest peak occurring around 35 minutes. The reflections are caused by the interaction of seismic waves with the ocean floor and subsurface layers, which have different acoustic properties. The profile is used to study the structure of the ocean floor and subsurface layers, and to estimate the depth of the ocean floor and the thickness of the subsurface layers.

The seismic reflection profile shown in Figure 1 is a typical example of a deep sea seismic reflection profile. It shows multiple reflections from the ocean floor and subsurface layers. The profile is characterized by a series of peaks and troughs, with the highest peak occurring around 35 minutes. The reflections are caused by the interaction of seismic waves with the ocean floor and subsurface layers, which have different acoustic properties. The profile is used to study the structure of the ocean floor and subsurface layers, and to estimate the depth of the ocean floor and the thickness of the subsurface layers.